A New Technique for Doppler Frequency Compensation and Estimation for High-speed Targets in Phase-Coded Radars

Alaa G. Zahra,[1] Wael Mehany,[1] Fathy M. Ahmed,[1] Ahmed Youssef ,[1] Mostafa Elsayed,[2] and Julien Le Kernec [2]

[1] *Radar Department, Military Technical College, Cairo, Egypt*

[2] *James Watt School of Engineering, University of Glasgow, UK*

Email: mostafa.elsayed@glasgow.ac.uk

Moving targets are a real threat to pulse compression radars, especially those operating with Doppler-intolerant waveforms. As the Doppler frequency increases, the radar system performance degrades accordingly. In the case of high-speed targets, the Doppler frequency is high enough to distort the received signal, and consequently, the matched filter output is distorted. Therefore, no target information could be extracted. In this paper, we introduce a new Doppler compensation (DC) and estimation technique for phase-coded pulse compression radars to allow the detection of high-speed targets. Moreover, their Doppler frequency value is estimated without ambiguity from one burst and without the need for a range-Doppler module. In addition, the proposed method does not require a synchronization system to perform its function. As such, the implementation of the proposed method is simple and inexpensive. The performance evaluation of the new method shows its superiority in compensation and estimation when examined under higher Doppler frequency and noise compared to a conventional radar.

Introduction: Pulse compression (PC) technique is one of the most fundamental principles in pulsed radar signal processing as it allows good range resolution beside transmitting high average power for long range detection. PC is applied to two major classes of waveforms, frequency-modulated (FM) and phase-modulated (PM) signals. A PM pulse is a sequence of time segments, referred to as chips, such that the phase of each chip belongs to a set of specific values. These signals are known to have a perfect autocorrelation function (ACF), a wide bandwidth, and a simple implementation. On the other side, PM waveforms suffer from high Doppler values that appear at the matched filter (MF) output as time-sidelobe level. The higher the Doppler value, the more degradation occurs. As a result, the probability of false alarm P_fa increases while the probability of detection P_D decreases[1].

Nowadays, the detection of high-speed targets such as fighter aircraft and artillery missiles has gained much attention as one of the most critical topics in current technology. In fact, the detection of these types of targets by traditional radars is a challenging operation, specially for radars using Doppler-intolerant signals, the effect of the high Doppler frequency is severe and distorts the received echo. Therefore, the MF output is severely degraded and the target information is lost. The effect of high-speed targets on Doppler insensitive waveforms such as the linear FM signals is serious, as it causes range/Doppler migration and velocity ambiguity [2].

Regarding Doppler sensitive signals, many studies have been presented to compensate the Doppler frequency effect on PM waveforms. In [3], the author presents a Doppler compensation (DC) method for compensating the Doppler frequency influence on the binary phase-coded signals. It is based on a Doppler shift emulator module with a multi-channel correlation . The correlator outputs are compared to each other and the maximum is registered. The limitation of this method is that the multichannel correlation requires large hardware resources, resulting in a longer computational time and a costlier system. Moreover, the Doppler information is lost. Authors in [4] succeeded to compensate the Doppler effect on the complementary binary phase-coded signals. However, their algorithm depends on multiplying every sample at index n by the conjugate of the adjacent sample at $n+1$ to get the desired compensated binary code. This algorithm requires generating a new sequence of length N for every desired binary sequence of length N-1. For example, Barker code 5 requires transmitting a new sequence of 6 samples as $\{1, 1, 1, 1, -1, -1\}$. Therefore, the operation of generating a new code becomes complicated as the desired code length increases. In addition, the Doppler information is lost. In [5], the authors presented a new method to recover a binary phase-coded waveform and overcome the Doppler intolerance at the expense of Doppler information. As such, the authors relied on other waveforms to get the Doppler value, and therefore the complexity of the system is increased. These studies propose techniques to compensate the Doppler effect at modest values regarding targets moving with normal speed.

In this article, we introduce a new Doppler compensation and estimation (DCE) method for high-speed targets. The proposed technique aims to compensate Doppler frequency effect of high-speed targets on the received PM signal. Subsequently, the MF outputs will be detectable. As the Doppler information is lost during the DC operation, another process is done for estimating the Doppler value. The substantial advantage in our method is that no synchronization system is needed for predicting the target arrival time, which makes its implementation simple and inexpensive. Another interesting feature, we can determine the high-speed target from one burst without the need for a range-Doppler module, which minimizes the processing time and the implementation resources, as it is important when dealing with this target type. Our method presents a new framework for high-speed targets radar signal processing.

This paper is organized as follows: first, the methodology of the proposed technique is introduced with the mathematical details followed by the the simulation results, and finally the paper discussion and the future work are presented.

Main idea: The block diagram of the proposed algorithm is shown in Fig. 1, it consists of two routes; the first route is devoted to the DC process, and the second route is for estimating the Doppler frequency. $X_r[n]$ denotes the received signal. The Doppler compensation and esti-

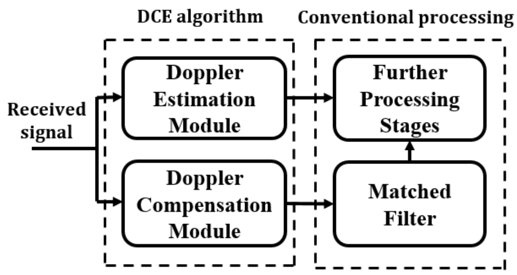

Fig 1 *The block diagram of the proposed DCE algorithm.*

mation (DCE) operation depends on transmitting two successive pulses. The first pulse is the PM pulse, and the second one is the unmodulated pulse, as shown in Fig. 2. The two pulses are equal in duration τ with N_p samples, and pulse repetition time (PRT), T_r, with N_t samples.

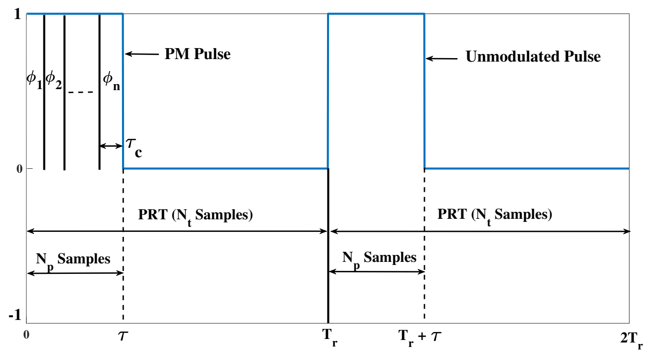

Fig 2 *The transmitted waveform.*

Doppler compensation algorithm: The DC approach depends on sample-by-sample element-wise multiplication, where every sample of k^{th} order in the first PRT is multiplied by the conjugate of its equivalent in the second PRT. As shown in Fig. 3, the DC block diagram involves

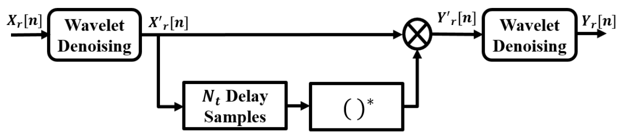

Fig 3 *The block diagram of the DC algorithm.*

a single delay line that has a value of N_t delay elements, a conjugate module, and a multiplier. The output after the multiplication process is a PM signal with a constant phase difference after Doppler suppression (details are explained later on), which is similar to the MF signal stored replica. Assuming that one sample for each subpulse is considered such that the sampling period T_s equals the subpulse duration τ_c, the transmitted waveform in the discrete time domain can be represented as follows:

$$X_t[n] = x_{t_1}[n] + x_{t_2}[n - N_t] \tag{1}$$

Where $x_{t_1}[n]$ and $x_{t_2}[n]$ are the phase-coded and the unmodulated pulses, respectively. The transmitted pulses waveforms are defined as:

$$x_{t_1}[n] = \begin{cases} \sum_{k=0}^{N_p-1} a_{t_1} e^{j\phi_k} & \delta[(n - kT_s)] \\ 0 & , N_p \leq k < N_t - 1 \end{cases} \tag{2}$$

$$x_{t_2}[n] = \begin{cases} \sum_{k=0}^{N_p-1} a_{t_2} \delta[(n - kT_s)] & \\ 0 & , N_p \leq k < N_t - 1 \end{cases} \tag{3}$$

Where ϕ_k represents the phase for each time segment, a_{t_1} is the amplitude of the PM pulse, a_{t_2} is the amplitude of the unmodulated pulse, and $\delta[n]$ is the Dirac delta function.

At the receiver, and after the down-conversion and digitizing of the received signal $X_r[n]$, the discrete signals $x_{r_1}[n]$ and $x_{r_2}[n]$ are the baseband target returns from the modulated and unmodulated pulses, respectively, that can be written as:

$$X_r[n] = x_{r_1}[n - N_d] + x_{r_2}[n - N_t - N_d] \tag{4}$$

Where N_d is the target delay such that $N_p \leq N_d \leq N_t$. The signals $x_{r_1}[n]$ and $x_{r_2}[n]$ are explicitly defined as:

$$x_{r_1}[n] = \sum_{k=0}^{N_p-1} a_{rn_1} e^{j(\phi_k + 2\pi f_d(n - N_d - kT_s))} + N_1[n] \tag{5}$$

$$x_{r_2}[n] = \sum_{k=N_t}^{N_t+N_p-1} a_{rn_2} e^{j(2\pi f_d(n - N_d - kT_s) + \theta)} + N_2[n] \tag{6}$$

Where a_{rn_1} and a_{rn_2} are the sample amplitudes of the PM and unmodulated pulses respectively, $N_1[n]$ and $N_2[n]$ represent the added noise for each pulse, respectively, where f_d is the target Doppler frequency, and θ is the phase difference between the two received echoes.

In Fig. 4, a received PM pulse, nested-Barker of 507 samples, of a target at time T_1 is shown. Fig. 4(a) shows the distortion in received signal as the result of a high-speed target. In this case, no information could be extracted at the MF output. After the proposed compensation process, however, the PM pulse is recovered as shown in Fig. 4(b), and the MF is then valid for the detection process. Since the received signal is contaminated with noise, whose variance increases because of the multiplication operation. Wavelet denoising algorithm is one of the non-expensive solutions for minimizing the noise level at the first stage and also after the multiplication process. Wavelet analysis separates the original signal into various frequency components, and examines each component separately. Depending on the frequency, the basis functions of the wavelet transform are scaled. There are several varieties of wavelets. They have diverse qualities and come from various wavelet families [6]. The Haar wavelet is used in the proposed scheme.

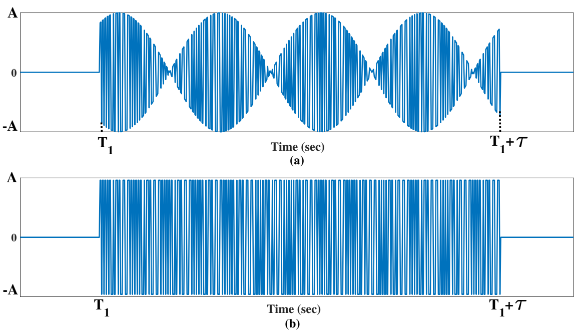

Fig 4 *The received PM pulse (a) Before the DC algorithm. (b) After the DC algorithm.*

Applying the algorithm explained in Fig. 3, the multiplier output Y'_r is represented as:

$$Y'_r[n] = X'_r[n] \odot X'^*_r[n - N_t] \tag{7}$$

Where X'_r is the wavelet-denoised version of X_r, $(^*)$ denotes the complex conjugate operation, and $\odot$ refers to the element-wise multiplication. The multiplier output for any two samples separated by N_t samples (because of the delay line) will be modeled as:

$$Y'_r[n] = (a'_{rn_1} e^{j(\phi_k + 2\pi f_d(n - N_d)T_s)} + a_{n_1} N_1[n]) \odot \\ (a'_{rn_2} e^{j(2\pi f_d(n - N_d - N_t)T_s + \theta)} + a_{n_2} N_2[n])^* \tag{8}$$

Where a'_{rn_1}, a'_{rn_2}, a_{n_1}, and a_{n_2} are the amplitudes of the two pulses samples and the two added noise samples after the wavelet denoising stage, respectively. The expression in (8) can be simplified as:

$$Y'_r[n] = (a'_{rn_1} e^{j(\phi_k + 2\pi f_d nT_s + \theta_1)} + a_{n_1} N_1[n]) \odot \\ (a'_{rn_2} e^{j(2\pi f_d nT_s + \theta_2)} + a_{n_2} N_2[n])^* \tag{9}$$

Where $\theta_1 = -2\pi f_d N_d T_s$, and $\theta_2 = -2\pi f_d (N_d + N_t)T_s + \theta$. The output after element-wise multiplication is:

$$Y'_r[n] = a'_{rn_1} a'^*_{rn_2} e^{j(\phi_k + 2\pi f_d nT_s + \theta_1)} e^{-j(2\pi f_d nT_s + \theta_2)} \\ + a'_{rn_1} a^*_{n_2} e^{j(\phi_k + 2\pi f_d nT_s + \theta_1)} N_2^*[n] \\ + a_{n_1} a'^*_{rn_2} N_1[n] e^{-j(2\pi f_d nT_s + \theta_2)} + a_{n_1} a^*_{n_2} N_1[n] N_2^*[n] \tag{10}$$

After some simplifications, the expression represented in (10) can be written as:

$$Y'_r[n] = a'_{rn_1} a'^*_{rn_2} e^{j\phi_k} e^{j(\theta_1 - \theta_2)} + a'_{rn_1} a^*_{n_2} e^{j(\phi_k + 2\pi f_d nT_s + \theta_1)} \\ N_2^*[n] + a_{n_1} a^*_{n_2} N_1[n] N_2^*[n] + a_{n_1} a'^*_{rn_2} N_1[n] e^{-j(2\pi f_d nT_s + \theta_2)} \tag{11}$$

The output is fed into wavelet denoising filter; the result is written as:

$$Y_r[n] = a''_{rn_1} a'^{*\prime}_{rn_2} e^{j\phi_k} e^{j(\theta_1 - \theta_2)} + a''_{r_1} a^{*\prime}_{n_2} e^{j(\phi_k + 2\pi f_d nT_s + \theta_1)} N_2^*[n] \\ + a'_{n_1} a'^{*\prime}_{rn_2} N_1[n] e^{-j(2\pi f_d nT_s + \theta_2)} + a'_{n_1} a^{*\prime}_{n_2} N_1[n] N_2^*[n] \tag{12}$$

Where Y_r is the denoised multiplier output, and the second $(')$ on the sample amplitudes denotes the effect of the second wavelet denoising algorithm.

In (12), the first term is the Doppler-compensated phase-modulated term with a constant phase difference. This term is close to the replica signal in the MF. The amplitude and the phase constant are mainly depend on the target parameters and channel conditions. The effect of Doppler frequency appears in the next two terms multiplied with noise. It should be noted that the Doppler effect is an additive effect not a multiplicative one as before. Therefore, its effect on the algorithm performance is significantly decreased. The last term is only noise which is already reduced after the wavelet process.

Doppler frequency estimation: Since the Doppler information at the output of the proposed DC module is lost, we rely on another module to get the value of the Doppler, namely, the Doppler estimation (DE) module. The DE method depends mainly on the unmodulated pulse, which holds the Doppler signal contaminated with noise. After the wavelet filter, the Fast Fourier Transform (FFT) algorithm is used to calculate the pulse spectral coefficients. Doppler value is calculated based on the index of spectrum peak D_n, which corresponds to the Doppler bin number. By taking the average value of the Doppler bin over N_r iterations, the Doppler value f_{d_e} is estimated as indicated in (13).

$$f_{d_e} = D_b \sum_{n=1}^{N_r} \frac{D_n}{N_r} \tag{13}$$

Where D_b is the Doppler resolution. It also should be noted that, the necessary condition for Doppler extraction from oneburst is that the Doppler value is high enough to complete at least one cycle within the pulse width τ as shown in (14).

$$f_{d_{min}} \geq \frac{1}{\tau} \tag{14}$$

In our module, the fast time sampling, $f_s = 1/\tau_c$, is considered when calculating the spectral coefficients for the received signal. Therefore, the maximum received Doppler frequency $f_{d_{max}}$ of a target is limited by sampling frequency as indicated in (15).

$$f_{d_{max}} \leq \frac{f_s}{2} \tag{15}$$

Table 1. Simulated parameters

Parameter	Value
Modulation type	BPSK Nested Barker(13*13*3)
Range resolution	100 m
Operating wavelength λ	0.15 m
Pulse repetition frequency f_r	296 Hz
Sampling frequency f_s	1.5 MHz
PRT	3.38 ms
Duty cycle	10%
τ	338.169 μs
$fd_{min} = 1/\tau$	2958 Hz
$\tau_c = T_s$	0.667 μs
N_t	5070 $samples$
N_p	507 $samples$
Doppler resolution cell $D_b = f_s/N_t$	296Hz
R_t	100 km
f_1, f_2, f_3	29600 Hz, 9472 Hz, 59200 Hz

Simulation and analysis: The performance evaluation is done by the well-known curve that combines, P_D and SNR at a given probability of false alarm (P_{fa}). We can call it "PD curve". A moving target is simulated at different f_d values at a given range R_t relying on the simulation parameters that are listed in Table 1.

To examine our new method using the PD curve, a constant false alarm rate (CFAR) processor is added after the MF to compute the adaptive threshold. Note that, the proposed algorithm is added as a prepossessor module to the traditional radar processors (i.e MF and CFAR processors). Fig. 5 shows the PD curve for the proposed method and the traditional method at three different frequencies: f_1, f_2, and f_3. In our case, we analyze SNR with respect to PD for the given P_{fa} value of 10^{-6}. This value is a typical value in radar system. It is calculated by injecting noise only to the system and computing the K factor of CFAR that ensures the selected P_{fa} value. From the figure, the performance of the proposed technique is superior than the traditional radar processing method at all SNR values.

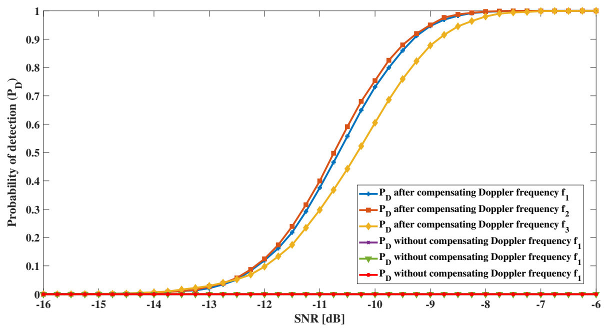

Fig 5 *PD curves for three frequencies with and without DC*

Fig. 6 shows the MF output with and without using the proposed algorithm for a moving target at range R_t and Doppler frequency $f_d = f_3$ at $SNR = 0$ dB. The outputs show that our DC method can detect target at its specified range without the effect of Doppler as in conventional MF output which is totally distorted.

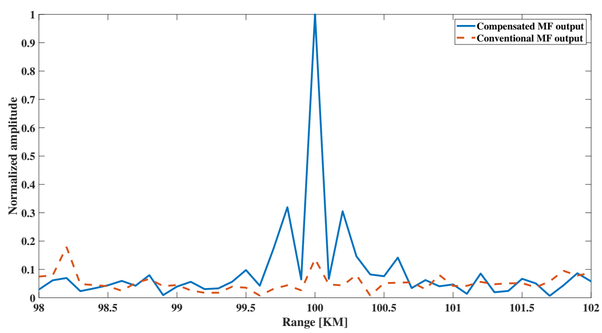

Fig 6 *The MF output With and without DC*

As a further assessment, the sensitivity of the proposed algorithm in estimating high Doppler values at different SNR values is evaluated. In Fig. 7, the three Doppler frequencies f_1, f_2, and f_3 are selected, such that they lie in the Doppler cells 100, 32, and 200, respectively. The estimated Doppler cell is obtained by calculating the average value of the estimated Doppler bin over 1000 iterations for every SNR value. From Fig. 7, the DE module has a promising output when $SNR \geq -9$ dB.

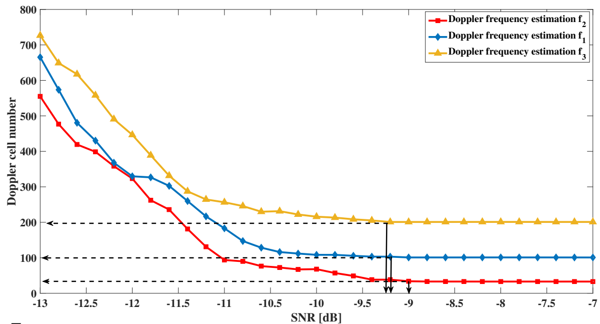

Fig 7 *Doppler Frequency estimation at different SNR values*

Discussion: The proposed DCE technique is mainly effective against high-speed targets whose Doppler frequencies are within the range specified by (14) and (15). In the case of low and intermediate target speeds, the traditional radar signal processing techniques will be adequate for extracting the target information. Therefore, our proposed algorithm could be used as a sub-module in a typical radar. The user could activate the module based on the situation and the expected threats.

Conclusion and future work: High-speed targets are a real threat for radar systems operating with phase-coded waveforms because they are categorized as Doppler-intolerant signals. As a result, their corresponding MF output is disfigured due to the dissimilarity between the received signal and the MF stored replica. Therefore, estimating the range and velocity of targets is almost impossible. The proposed method presents an effective solution for compensating the Doppler effect to recover the shape of the received signal, and then retrieve the well-known shape of the correlation at the MF output. In addition, the Doppler frequency information has been extracted using the Doppler estimation module using only one busrt. The analysis of our method showed that the performance of the radar system is significantly enhanced. Our future developments will include enhancing the performance of the proposed method by suppressing the sidelobes shown in 6, evaluating the robustness of the algorithm with multiple targets, and investigating the performance of the new method with different types of clutter.

References

1. Bhatt, T.D., Singh, S.P.: Non-coherent pulse compression waveforms. In: 2021 3rd International Conference on Signal Processing and Communication (ICPSC), , pp. 508–512. (2021)
2. Xu, L., Lien, J., Li, J.: Doppler–range processing for enhanced high-speed moving target detection using lfmcw automotive radar. IEEE Transactions on Aerospace and Electronic Systems 58(1), 568–580 (2022). doi:10.1109/TAES.2021.3101768
3. Matousek, Z., et al.: Doppler compensation for binary phase-coded radar signals in presence of noise jamming. In: 2016 17th International Radar Symposium (IRS), , pp. 1–4. (2016)
4. Li, W., et al.: Doppler compensation method for the complementary phase-coded signal. The Journal of Engineering 2019(21), 7521–7524 (2019). doi:10.1049/joe.2019.0379
5. Youssef, A., et al.: A novel framework for combining multiple radar waveforms using time compression overlap-add. IEEE Transactions on Signal Processing 69, 4371–4384 (2021). doi:10.1109/tsp.2021.3094050
6. Ouahabi, A.: A review of wavelet denoising in medical imaging. In: 2013 8th International Workshop on Systems, Signal Processing and their Applications (WoSSPA), , pp. 19–26. (2013)
7. Richards, M.A., Scheer, J.A.: Principles of modern radar. SciTech Pub. (2014)